

# Discovery of two bright DO-type white dwarfs <sup>★</sup> †

Nicole Reindl,<sup>1</sup> ‡ S. Geier,<sup>2</sup> R. H. Østensen<sup>3</sup>

<sup>1</sup>*Department of Physics and Astronomy, University of Leicester, University Road, Leicester LE1 7RH, UK*

<sup>2</sup>*Institute for Physics and Astronomy, University of Potsdam, Karl-Liebknecht-Str. 24/25, D-14476 Potsdam, Germany*

<sup>3</sup>*Department of Physics, Astronomy and Materials Science, Missouri State University, Springfield, MO 65897, USA*

Accepted XXX. Received YYY; in original form ZZZ

## ABSTRACT

We discovered two bright DO-type white dwarfs, GALEX J053628.3+544854 (J0536+5448) and GALEX 231128.0+292935 (J2311+2929), which rank among the eight brightest DO-type white dwarfs known. Our non-LTE model atmosphere analysis reveals effective temperatures and surface gravities of  $T_{\text{eff}} = 80000 \pm 4600$  K and  $\log g = 8.25 \pm 0.15$  for J0536+5448 and  $T_{\text{eff}} = 69400 \pm 900$  K and  $\log g = 7.80 \pm 0.06$  for J2311+2929. The latter shows a significant amount of carbon in its atmosphere ( $C = 0.003^{+0.005}_{-0.002}$ , by mass), while for J0536+5448 we could derive only an upper limit of  $C < 0.003$ . Furthermore, we calculated spectroscopic distances for the two stars and found a good agreement with the distances derived from the Gaia parallaxes.

**Key words:** stars: white dwarfs – stars: atmospheres – stars: abundances

## 1 INTRODUCTION

About every fifth intermediate mass star will turn into a star with a H-deficient atmosphere in its late stage of stellar evolution. There are various scenarios that can produce H-deficient stars, such as (very) late thermal pulses (e.g., Iben et al. 1983; Althaus et al. 2005), the merger of two white dwarfs (Zhang & Jeffery 2012a,b), or the late hot flasher scenario (Miller Bertolami et al. 2008). Once these H-deficient stars enter the white dwarf cooling sequence, their atmospheres are dominated by He. The earliest type of these He-dominated white dwarfs corresponds to the DO spectral type. These stars have effective temperatures ( $T_{\text{eff}}$ ) between 45 000 and 200 000 K, with the hot DO white dwarfs showing strong He II lines, whereas in the spectra of cool DO white dwarfs He I lines can also be seen (Sion 2011).

DO-type white dwarfs cover a huge luminosity interval from up to  $10^4$  times the solar luminosity, when they have just entered the white dwarf cooling sequence, down to only  $0.1 L_{\odot}$  when reaching to the DB-spectroscopic region. This evolutionary phase is quite short-lived ( $\approx 2$  million years, Althaus et al. 2009), thus less than 100 DO white dwarfs are currently known.

The detection of more of these stars is important for the construction of a reliable hot end of the white dwarf luminosity function

(WDLF). Its hot end suffers from low number statistics, i.e., the high luminosity bins ( $-0.5 < M_{\text{bol}} < 4.0$ , corresponding to white dwarfs with  $T_{\text{eff}} > 50000$  K) of the hot WDLF of Krzesiński et al. (2009) contain only one to 29 objects each. Since the shape of the WDLF quantitatively reflects the cooling behaviour of the white dwarf population as a whole, it is an excellent tool for constraining the properties of particles emitted by the white dwarfs. The cooling process of hot and luminous white dwarfs is dominated by the radiation of neutrinos, thus, the shape of the hot end of the WDLF strongly constrains the magnetic dipole moment of the neutrino Miller Bertolami (2014). Moreover, it offers the opportunity to check for the possible existence of the axion, a proposed but not yet detected type of weakly interacting particles (Miller Bertolami et al. 2014).

DO-type white dwarfs with  $T_{\text{eff}} = 58000 - 85000$  K are found to display high abundances of trans-iron elements (Hoyer et al. 2017, 2018). Therefore, high resolution ultra-violet (UV) spectra of DO white dwarfs, in which a wealth of metal lines can be detected, enables us to study the chemical evolution of these stars and to put constraints on possible progenitors and progeny. Furthermore, hot white dwarfs serve as stellar laboratories to derive atomic data for highly ionized species of trans-iron elements (Rauch et al. 2012, 2014b,a, 2015a,b, 2016, 2017a,b).

Last but not least, hot white white dwarfs have recently found a new use in the fundamental physics community. They potentially allow us to directly observe variations in fundamental constants, i.e., the fine structure constant  $\alpha$ , at locations of high gravitational potential. Such a variation manifests itself as shifts in the observed wavelengths of absorption lines, when compared to laboratory wavelengths. This effect is larger for metals with more protons (higher atomic number) and higher ionization energy. Thus, Fe v

\* Based on observations collected at the German-Spanish Astronomical Center, Calar Alto, jointly operated by the Max-Planck-Institut für Astronomie Heidelberg and the Instituto de Astrofísica de Andalucía (CSIC).

† Based on observations made with the William Herschel Telescope and the Isaac Newton Telescope operated on the island of La Palma by the Isaac Newton Group of Telescopes in the Spanish Observatorio del Roque de los Muchachos of the Instituto de Astrofísica de Canarias.

‡ E-mail: nr152@le.ac.uk

and Ni v that can be found in high-resolution UV spectra of hot white dwarfs are particularly well suited for this purpose (Berengut et al. 2013; Preval et al. 2015; Bainbridge et al. 2017).

The Hubble Space Telescope (HST) is currently the only telescope that can be used to obtain UV spectra for the above mentioned proposes. Thus, bright white dwarfs ( $V < 16$  mag) are a requisite to gain a high signal to noise (S/N), high-resolution UV spectrum, necessary to resolve the weak metal lines in hot white dwarfs.

In this letter we report the discovery of two such bright DO white dwarfs, GALEX J053628.3+544854 and GALEX 231128.0+292935 (hereafter J0536+5448 and J2311+2929). Since most of the DO white dwarfs have been discovered within the Solan Digital Sky Survey, the majority of DO type white dwarfs are significantly fainter (mean V magnitude is 17.3 mag). The two stars presented here have V magnitudes of  $15.186 \pm 0.062$  (J0536+5448) and  $15.491 \pm 0.040$  (J2311+2929, Henden et al. 2016) and therefore they rank among the eight brightest DO-type white dwarfs known. The only six DO white dwarf brighter than those two are HZ 21, HS 0111+0012, RE 0503–289, PG 0109+111, PG 0038+199, and PG 1034+001.

## 2 SPECTROSCOPIC OBSERVATIONS

We observed J0536+5448 and J2311+2929 during surveys exploring candidate dB stars for the Kepler mission, selected from the GALEX survey. In August 2010 J0536+5448 was observed twice at the William Herschel Telescope using the Intermediate Dispersion Spectrograph and Imaging System (ISIS) with the R600B grating ( $R \approx 4000$ ), covering the wavelength range 3500 – 5200 Å. J0536+5448 was again observed at the Isaac Newton Telescope (INT) February 2011 using the Intermediate Dispersion Spectrograph (IDS) with the R400B grating ( $R \approx 1500$ ) covering the wavelength range of 3500 – 9000 Å. J2311+2929 was observed with the same set-up at the INT in July 2013. Based on these spectra we assigned the spectral type DO.

To obtain high S/N spectra suitable for a precise spectral analysis, we performed spectroscopic follow-up in October/November 2014 at the Calar Alto 3.5 m telescope (ProgID H14-3.5-022) using the TWIN spectrograph and a slit width of 1.2 arcsec. We used the grating No. T08 for the blue channel and No. T04 for the red channel (dispersion 72 Å/nm, covering the wavelength range 3500 – 7300 Å). The resolution of the spectra is 1.8 Å. We obtained four spectra of J0536+5448 and seven spectra of J2311+2929 with exposure times of 20 minutes to achieve a S/N > 100. The spectra were taken in three consecutive nights. After each spectrum, we required ThAr wavelength calibration. The data reduction was done by using IRAF<sup>1</sup>. We did not perform flux calibration to our data.

The co-added TWIN spectrum of J0536+5448 reaches a S/N (interpreted as mean/standard deviation, measured in the region 6000 – 6250 Å) of 120 and displays He II  $\lambda\lambda$  4339, 4542, 4686, 4859, 5411, 6560 Å, He I  $\lambda\lambda$  5876, 7065 Å. The co-added TWIN spectrum of J2311+2929 reaches a S/N of 200 and additionally shows lines of He I  $\lambda\lambda$  4472, 4922, 5016, 6678 Å and

C IV  $\lambda\lambda$  4646 – 4660, 5814, 5803 Å. To check for radial velocity variations, we measured the radial velocities of the identified lines by fitting a set of mathematical functions (Gaussians, Lorentzians, and polynomials) to the identified spectral lines using SPAS (Spectrum Plotting and Analysing Suite, Hirsch 2009). None of the two stars displays any radial velocity variations larger than 20 km/s, corresponding to the standard deviation of the individually measured radial velocities.

## 3 SPECTRAL ANALYSIS

### 3.1 Effective temperatures and surface gravities

We derived the effective temperatures and surface gravities of the two stars by means of a  $\chi^2$  minimization technique with SPAS, which is based on the FITSB2 routine (Napiwotzki 1999). The fit is based on the co-added TWIN spectra of the two stars and the model grid of Reindl et al. (2014), which was calculated with the Tübingen non-LTE Model-Atmosphere Package (TMAP, Werner et al. 2003, 2012; Rauch & Deetjen 2003). To account for the spectral resolution of the TWIN observations, the synthetic spectra were convolved with Gaussians ( $FWHM = 1.8$  Å). We fitted the He II  $\lambda\lambda$  4339, 4542, 4686, 4859, 5411, 6560 Å, He I  $\lambda\lambda$  5876, 7065 Å, and for J2311+2929 additionally He I  $\lambda\lambda$  4472, 4922, 5016, 6527 Å. For J0536+5448 we derived  $T_{\text{eff}} = 80000 \pm 4600$  K and  $\log g = 8.25 \pm 0.15$ , and for J2311+2929 we found  $T_{\text{eff}} = 69400 \pm 900$  K and  $\log g = 7.77 \pm 0.06$ . The errors represent the statistical one sigma uncertainty on  $T_{\text{eff}}$  and the three sigma uncertainty on  $\log g$ .

In Fig. 1 we show the fits to the He lines of the co-added TWIN spectra of the two stars. For J0536+5448 (left panel of Fig. 1), the He II lines are nicely reproduced by the best fit model (red), but the theoretical He I  $\lambda$  7065 Å is too shallow and the He I  $\lambda$  5876 Å too deep. We also show in this figure the models which are 4600 K (error from the  $\chi^2$  fit) hotter (green) and 4600 K cooler (blue). While the cooler model reproduces best the He I  $\lambda$  7065 Å, the hotter one matches He I  $\lambda$  5876 Å. For J2311+2929 (left panel of Fig. 1), the He I lines are reproduced well, but the line cores of He II  $\lambda\lambda$  5411, 6560 Å are too shallow in the pure He model (light blue).

As a next step, we calculated TMAP model grids, which also include opacities of C, N, and O. The statistics of our model atoms used for the model atmosphere calculations are summarized in Table 1. The addition of C in the models does not affect the theoretical He I and He II (see also Reindl et al. 2014). We also demonstrate this in left panel of Fig. 1, where a HeC model (dashed pink) is compared to the pure He model (light blue), both with  $T_{\text{eff}} = 69400$  K and  $\log g = 7.77$ . Comparing these models to our HeCNO models, we find that the line cores of He II  $\lambda\lambda$  5411, 6560 Å become deeper for increasing abundances of N and O. In case of J2311+2929 this indeed solves the problem of the observed too deep He II  $\lambda\lambda$  5411, 6560 Å lines (red line in the left panel of Fig. 1 represents the HeCNO model). We then repeated the  $\chi^2$  fit for J2311+2929 based on the HeCNO models. We found that  $T_{\text{eff}}$  is not affected by the inclusion of CNO (the derived  $T_{\text{eff}}$  is mainly a result of the strengths of the He I lines, which are not affected by the inclusion of CNO) and that the derived surface gravity increases only by 0.03 dex. We will therefore adopt in following, one sigma errors on  $T_{\text{eff}}$  and three sigma errors on  $\log g$ .

<sup>1</sup> IRAF is distributed by the National Optical Astronomy Observatory, which is operated by the Associated Universities for Research in Astronomy, Inc., under cooperative agreement with the National Science Foundation.

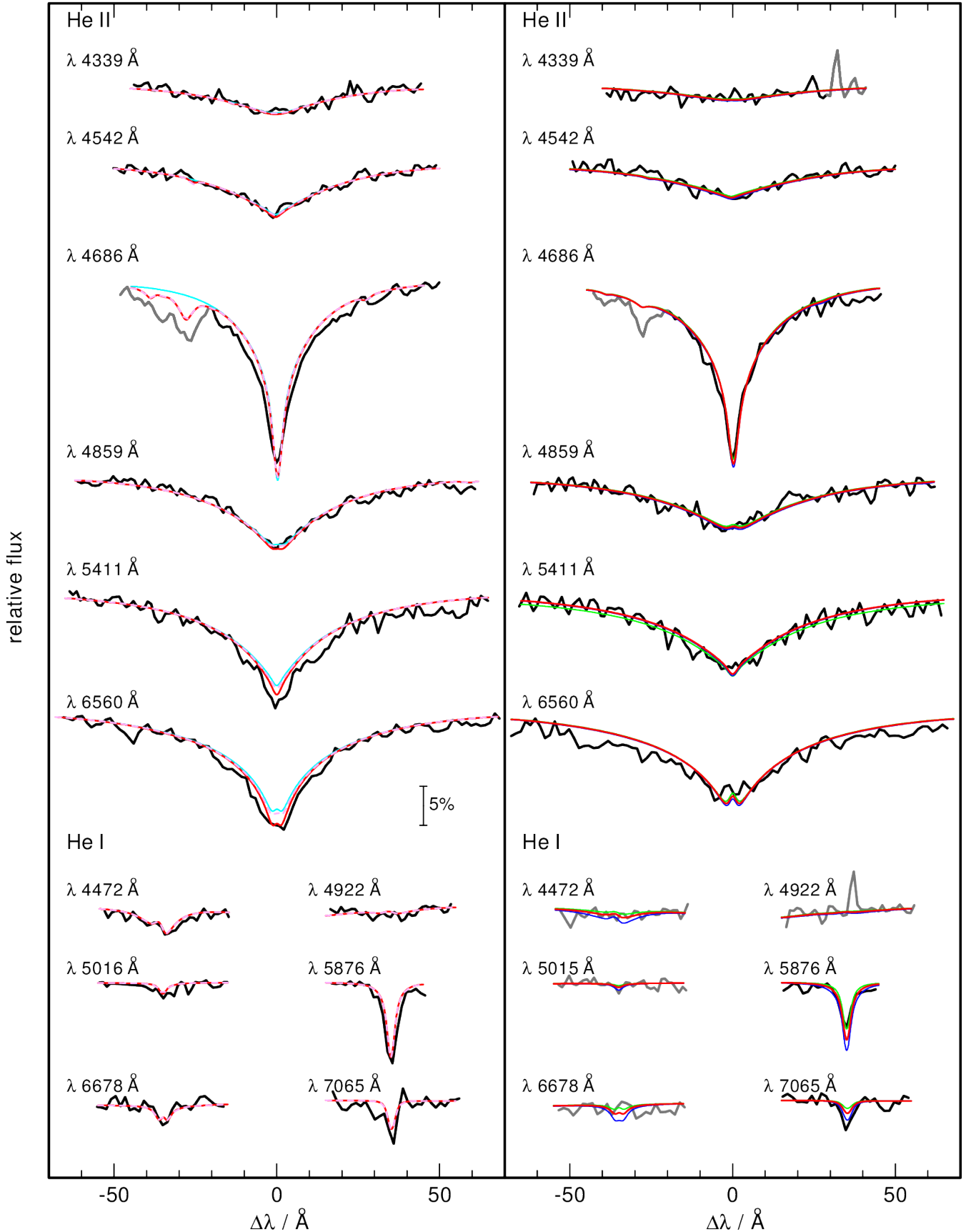


**Figure 1.** Coadded and normalized TWIN spectra (black) of J2311+2929 (left) and J0536+5448 (right). In the left panel the impact of C, N, and O on the theoretical lines profiles is demonstrated (light blue: pure He model, dashed pink: HeC model, red: HeCNO model). In the right panel models with different  $T_{\text{eff}}$  are shown (red: 80000 kK, blue: 75400 kK, green: 84600 kK). Regions excluded from the  $\chi^2$  fit are shown in grey. The vertical bar indicates 5% of the continuum flux.

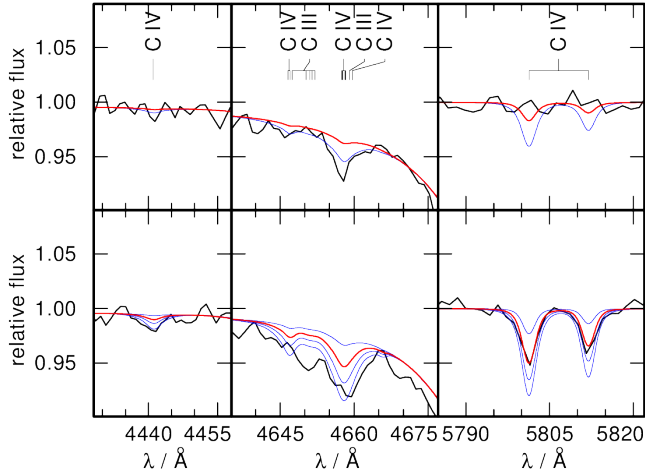


**Figure 2.** Determination of the C abundance of J2311+2929 (bottom panel) and the upper limit on the C abundance for J0536+5448 (upper panel). The red line indicates the (upper limit of) C abundance as derived from C IV  $\lambda\lambda$  5801, 5812 Å in the TWIN spectra. C abundances in the models for J2311+2929 are 0.001, 0.003, 0.005, and 0.008 and for J0536+5448 0.001 and 0.003 (mass fractions).

### 3.2 Carbon

For J2311+2929 the observed C IV  $\lambda\lambda$  5802, 5012 Å lines are well reproduced for  $C = 0.003$  (mass fraction), but not the absorption at 4646 – 4660 Å, which suggest  $C = 0.008$  (Fig. 2). Our models predict also C IV  $\lambda\lambda$  4441 Å. There is small absorption at this wavelength in the spectrum of J2311+2929, which however lies within the noise level of the spectrum, leaving the identification of this line uncertain. J0536+5448 does not show C IV  $\lambda\lambda$  5802, 5012 Å suggesting  $C < 0.001$ . The TWIN spectrum of this star, however, does show an absorption in the 4646 – 4660 Å region, which could be due to C IV  $\lambda\lambda$  4646 – 4660 Å and suggests  $C = 0.003$ . The IDS spectra of both stars are too noisy to allow the identification of C IV  $\lambda\lambda$  5802, 5012 Å, but both show the absorption at 4646 – 4660 Å, too.

This problem cannot be overcome with different combinations of  $T_{\text{eff}}$  and  $\log g$ . An increase of  $T_{\text{eff}}$  or a decrease  $\log g$  affects, however, C IV  $\lambda\lambda$  4646 – 4660 Å and C IV  $\lambda\lambda$  5802, 5012 Å in the same manner. For example, if  $T_{\text{eff}}$  is increased by 5000 K, or  $\log g$  decreased by 0.5 dex, this has a similar effect on those C lines as an increase of the abundance by 0.001. A decrease of  $T_{\text{eff}}$  by 5000 K, decreases the line strengths of all the C IV lines only minimally (the line strength of C III  $\lambda\lambda$  4650 – 4652 Å increases slightly in the cooler model for J2311+2929). Thus, a lower  $T_{\text{eff}}$  can also not account for the discrepancy of C abundance derived from the different C IV lines. We emphasize that both the C IV  $\lambda\lambda$  4646 – 4660 Å complex as well as the C IV  $\lambda\lambda$  5802, 5012 Å lines form at a similar part of the atmosphere ( $\log m \approx -2$ , where  $m$  is column mass that is measured from the outer boundary of the model atmospheres.), which means that it is unlikely that this problem could be solved by the inclusion of further metal opacities that would impact the temperature structure of the model atmosphere. So far, this problem has not been reported in the analysis of any other DO-type white dwarf. However, for some PG 1159 also only a poor simultaneous fit of the C IV  $\lambda\lambda$  4646 – 4660 Å and the C IV  $\lambda\lambda$  5802, 5012 Å lines is achieved. Similar to J0536+5448, the spectrum of the PG 1159 star HS 1517+7403 does show strong C IV  $\lambda\lambda$  4646 – 4660 Å lines while C IV  $\lambda\lambda$  5802, 5012 Å cannot be detected (Fig. 5 of Dreizler & Heber 1998). Another example is PG 0122+200 for which Werner

**Table 1.** Statistics of our model atoms.

	Ion	NLTE levels	Lines
He	i	29	69
	ii	20	190
	iii	1	–
C	ii	16	37
	iii	67	101
	iv	54	295
	v	1	0
N	iii	13	24
	iv	16	30
	v	14	35
	vi	1	0
O	iii	11	9
	iv	18	39
	v	17	25
	vi	14	33
	vii	1	0

**Table 2.** Atmospheric parameters of the two stars. Abundances are given in mass fractions.

	J0536+5448	J2311+2929
$T_{\text{eff}}$ [K]	$80000 \pm 4600$	$69400 \pm 900$
$\log g$ [ $\text{cm s}^{-2}$ ]	$8.25 \pm 0.15$	$7.80 \pm 0.06$
$C$	$< 0.003$	$0.003^{+0.005}_{-0.002}$
$N$	$< 0.005$	$< 0.005$
$O$	$< 0.01$	$< 0.01$

& Rauch (2014) could not precisely reproduce the observed central emission of C IV  $\lambda\lambda$  4659 – 4660 Å. Thus, an inaccuracy in the atomic data could be origin of this problem.

Another possible solution is a blend with an ultra-high excitation (uhe) absorption line, i.e., O VIII  $\lambda$  4658 Å. This line is seen in about every tenth DO-type white dwarf (Werner et al. 1995; Dreizler et al. 1995; Werner et al. 2014; Reindl et al. 2014), which are commonly referred to as hot-wind white dwarfs. The reason for the occurrence of these lines is not understood, but a photospheric origin can be excluded. On the other hand, the spectra of the hot wind white dwarfs are always accompanied by too broad and deep He II lines, which is not the case for our two stars. Also, should the (additional) line absorption around C IV  $\lambda\lambda$  4646 – 4660 Å stem from an uhe line it would be the first time that only this uhe line is observed.

### 3.3 Nitrogen and Oxygen

In our HeCNO models N IV  $\lambda$  4058 Å is the strongest of all nitrogen lines, followed by N IV  $\lambda$  6381 Å. In the hotter models ( $T_{\text{eff}} = 84600$  K) for J0536+5448, also the N V  $\lambda\lambda$  4604, 4620 Å doublet becomes slightly apparent. However, none of these lines are observed in the spectra. We derive an upper limit of  $N < 0.005$  for both stars. The strongest oxygen lines in our models are O III  $\lambda$  3962 Å followed by O IV  $\lambda$  3737 Å. Those lines are not visible in the spectra of our stars. We determine an upper limit of  $O < 0.01$  for both stars. We summarize the atmospheric parameters of the two stars in Table 2.



#### 4 MASSES, RADII, AND DISTANCES

J0536+5448 and J2311+2929 are included in Gaia data release 2 (Gaia Collaboration et al. 2016, 2018) and they have parallaxes of  $\pi = 4.488696620299169 \pm 0.08003018105955109$  and  $3.84995585215932 \pm 0.06101563607521435$ , respectively. An additional systematic error of the parallax due to uncertainties on the parallax zero-point and spatial correlations, of 0.1 mas is recommended by the Gaia team (see also Zinn et al. 2018). The resulting distances and height above or below the Galactic plane,  $z$ , are listed in Table 3.

By calculating the spectroscopic distance, we can now check for the consistency with the derived atmospheric parameters of the two stars. For that we firstly calculated absolute synthetic  $V$  band magnitude,  $M_V$ , according to Holberg & Bergeron (2006) using

$$M_V = -2.5 \log \frac{\int R^2 H_\lambda S_V(\lambda) d\lambda}{\int S_V(\lambda) d\lambda} + 73.6484,$$

where  $R$  is the radius of the star,  $H_\lambda$  the Eddington flux of our model spectrum, and  $S_V(\lambda)$  is the relative filter response modified for atmospheric transmission (Cohen et al. 2003). The spectroscopic distance can then be calculated via  $m_{V_0} - M_V = 5 \log(d[10pc])$ , where  $m_{V_0}$  is the observed  $V$  band magnitude after corrected for extinction. The reddening  $E_{B-V}$  of the stars was determined as follows. We obtained GALEX  $FUV$  and  $NUV$  magnitudes from Bianchi et al. (2014), 2MASS  $J$  and  $H$  magnitudes from Lawrence et al. (2013),  $u$ ,  $g$ ,  $r$ ,  $i$ , and  $z$  magnitudes for J2311+2929 from Ahn et al. (2012),  $g$ ,  $r$ ,  $i$ ,  $z$ ,  $W1$ , and  $W2$  magnitudes for J0536+5448 from Chambers et al. (2016) and Cutri & et al. (2014), and converted them into fluxes. Next, we normalized our best fit model atmosphere flux to the  $W1$  band flux for J0536+5448 and to the  $z$  band flux for J2311+2929. Using the reddening law of Fitzpatrick (1999) we then applied different values of  $E_{B-V}$  to the model spectrum until a good agreement with the multi-band photometry was achieved (Fig. 3). For J2311+2929 we found  $E_{B-V} = 0.06 \pm 0.03$  and  $E_{B-V} = 0.05 \pm 0.05$ . At the Gaia distances the Bayestar17 3D dust map (Green et al. 2014, 2018) gives  $E_{B-V} = 0.06 \pm 0.02$  for J2311+2929 and  $E_{B-V} = 0.12^{+0.11}_{-0.09}$  for J0536+5448. These values agree within the error limits, but for J0536+5448  $E_{B-V} > 0.10$  can be excluded, else the observed UV magnitudes cannot be reproduced.

To calculate the error on the  $M_V$ , the uncertainties of the stellar radius and the Eddington flux need to be considered. The uncertainty of the latter depends on  $T_{\text{eff}}$ ,  $\log g$ , as well as the metal content of the model. In principle, a higher  $T_{\text{eff}}$ , lower  $\log g$ , and higher metal content (flux is redistributed from the UV towards longer wavelengths) leads to a higher value of  $M_V$ . The metal content of our stars is unknown, but to estimate the effect of metals on the Eddington flux in the  $V$  band we obtained the model spectrum of the most metal-rich DO-type white dwarf RE 0503-289 from the German Astrophysical Virtual Observatory service TheoSSA<sup>2</sup>. Comparing the filter-weighted, integrated  $V$ -band fluxes of a pure He model with the one including metals (C, N, O, Si, P, S, Ca, Fe, Ni, Ge, Kr, Sn, Xe, Zn, and Ba), we find that the  $V$ -band flux would be underestimated by 4%. Masses and radii of DO-type white dwarfs were obtained from very late thermal pulse evolutionary tracks from Althaus et al. (2009, Fig. 4). The uncertainty of the radius of the star is determined by the errors on  $T_{\text{eff}}$  and  $\log g$ . The lack of the knowledge of the envelope mass adds an additional error of about 5%.

<sup>2</sup> <http://dc.zah.uni-heidelberg.de/theossa/q/web/form>

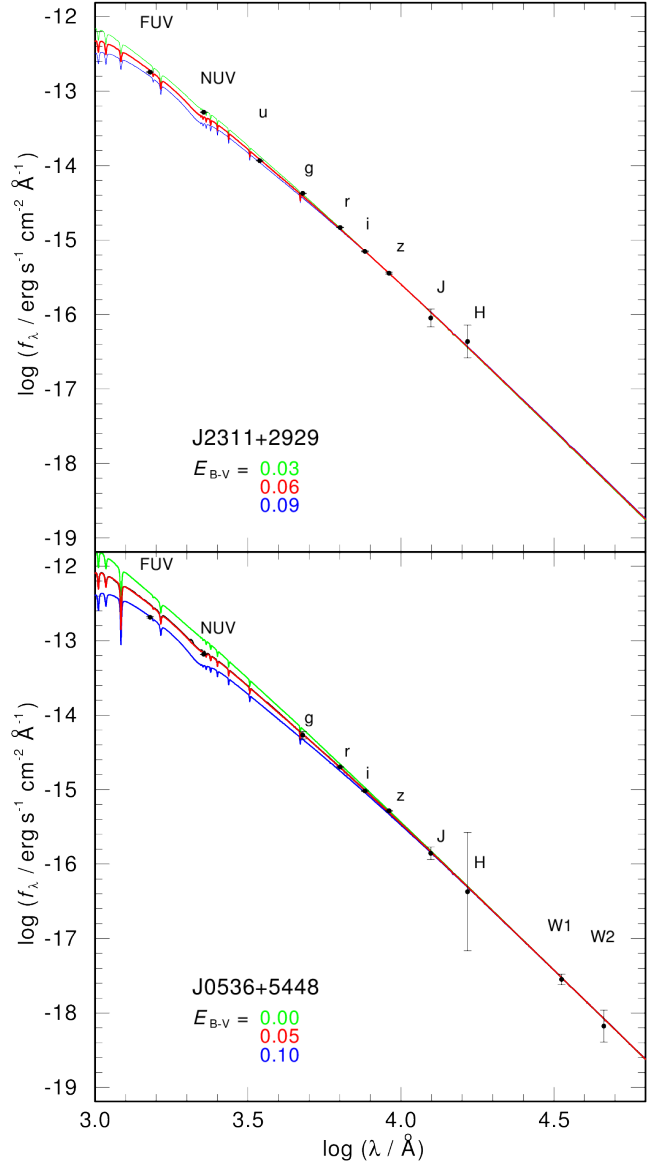


**Figure 3.** Determination of the reddening of J2311+2929 (upper panel) and J0536+5448 (lower panel).

The derived spectroscopic distances are listed in Table 2 and agree well with the Gaia distances. This confirms the reliability of our spectral analysis and the theoretical evolutionary calculations. In turn, we can now also calculate the radii of the two DO white dwarfs from the Gaia parallaxes, and using the mass-radius relationship of (Althaus et al. 2009) also determine their masses. The results are listed in Table 3. Note that the larger errors for J0536+5448 on the radii and masses derived from the Gaia data result from the larger uncertainty on  $T_{\text{eff}}$  and  $E_{B-V}$ .

#### 5 SUMMARY AND CONCLUSIONS

We reported about the discovery of two bright DO-type white dwarfs, J0536+5448 and J2311+2929, which rank among the eight brightest DO-type white dwarfs known. We performed a non-LTE spectral analysis of these two objects to derive their effective temperatures, surface gravities, C abundances (upper limit for J0536+5448), and upper limits for N and O. For J2311+2929 the

**Table 3.** Distances, height above/below the Galactic plane, masses, and radii as measured from spectroscopy and from Gaia parallaxes.

	J0536+5448		J2311+2929	
	Spec.	Gaia	Spec.	Gaia
$d$ [pc]	$156^{+59}_{-38}$	$223 \pm 9$	$235^{+44}_{-25}$	$260 \pm 11$
$z$ [pc]	$32^{+13}_{-7}$	$46 \pm 1$	$-112 \pm 11$	$-124 \pm 5$
$M$ [ $M_{\odot}$ ]	$0.820^{+0.080}_{-0.090}$	$0.630^{+0.165}_{-0.080}$	$0.597 \pm 0.020$	$0.575 \pm 0.005$
$R$ [ $R_{\odot}$ ]	$0.011^{+0.003}_{-0.001}$	$0.011^{+0.002}_{-0.001}$	$0.016 \pm 0.001$	$0.0174 \pm 0.0002$

observed line cores of He II  $\lambda\lambda 5411, 6560 \text{ \AA}$  are too deep when compared to the best fit pure He model. We could solve this problem by including CNO in our model atmosphere calculations. In J0536+5448 this problem is not apparent, likely because this star has lower metal content. We found a discrepancy of C abundance derived from C IV  $\lambda\lambda 5802, 5012 \text{ \AA}$  and C IV  $\lambda\lambda 4646 - 4660 \text{ \AA}$ , as the latter two lines suggest a 0.002-0.003 lower C abundance. An inaccuracy of the atomic data or a blend with an uhe line or another hitherto unknown line could be possible reasons. No lines of N and O could be detected, which demonstrates that low resolution optical spectra are not suited to detect and derive abundances of those elements. The atmospheric parameter of the two stars are summarized in Table 2.

Furthermore, we have determined the reddening and spectroscopic distances of the two stars. We found that our derived values for  $E_{B-V}$  agree within the error limits with those from the Bayestar17 3D dust map. We also find a good agreement of the spectroscopic distances, masses, and radii with those derived from Gaia parallaxes (Table 3). This confirms the reliability of our spectral analysis with the statistical one sigma uncertainty on  $T_{\text{eff}}$  and a three sigma error on  $\log g$ .

In Fig. 4 we show the locations of the newly discovered DO white dwarfs in the  $\log T_{\text{eff}} - \log g$  plane compared to very late thermal pulse evolutionary tracks of Althaus et al. (2009). The black lines indicate when the initial C abundance has dropped by a factor of two (solid line) and a factor of ten (dashed line) as predicted by Unglaub & Bues (2000). This explain why J2311+2929 still shows some C and J0536+5448 does not. Figure. 4 also shows the locations of the three DO white dwarfs, RE 0503-298, WD 0111+002 and PG 0109+111, studied by Hoyer et al. (2017, 2018). These stars are located close to the positions of our two bright DO white dwarfs, therefore it seems likely that J0536+5448 and J2311+2929 display high abundances of trans-iron elements, too. Both stars are very bright in the UV (Fig. 3, thus, they are excellent objects for follow-up observations in the ultra-violet to search for trans-iron group elements.

Another interesting point that becomes obvious from Fig. 4, is that J0536+5448 ranks amongst the most massive DO white dwarfs. Comparing the mass obtained from the Gaia parallax with the spectroscopic mass, we obtain a mass range of  $0.730 - 0.795 M_{\odot}$ . Because the theoretical variation of the fine structure constant  $\alpha$  with gravity is expected to increase with the compactness ( $M/R$ ) of an object, the detection of Fe v and Ni v lines in the spectrum of J0536+5448 would be especially interesting. We note that the compactness of J0536+5448 could exceed the ones in the sample of Bainbridge et al. (2017) by a factor of 1.4, suggesting that if  $\alpha$  exhibits a gravitational dependence the effect could be notably larger than the previous measurements. For example, if we assume for demonstrational purposes that the result from Berengut et al.

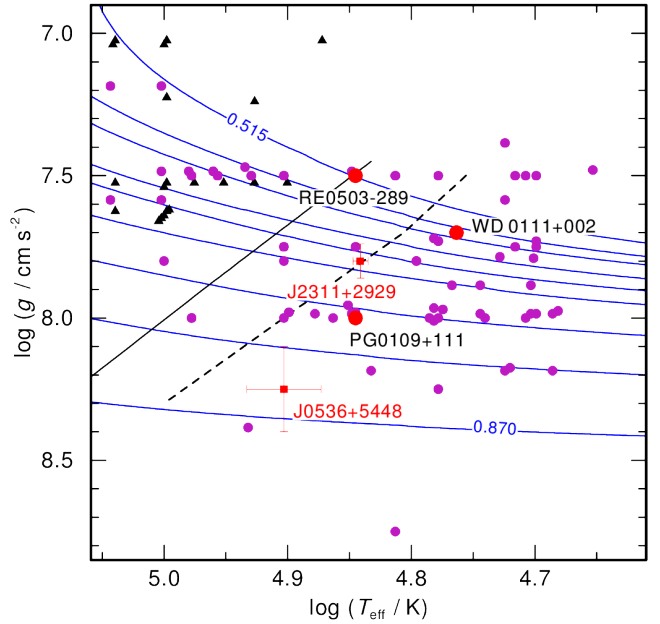


**Figure 4.** Locations of the newly discovered DO white dwarfs (red squares) and other known DO white dwarfs (purple dots, Reindl et al. 2014; Werner et al. 2014; Hügelmeier et al. 2006; Dreizler & Werner 1996, red dots Hoyer et al. 2017, 2018) and PG 1159 stars (black triangles, Werner et al. 2014; Gianninas et al. 2010; Werner & Herwig 2006; Schuh et al. 2008) in the  $\log T_{\text{eff}} - \log g$  plane compared to very late thermal pulse evolutionary tracks (solid lines, the lowest and highest mass tracks are labeled with stellar masses, intermediate tracks correspond to 0.530, 0.542, 0.565, 0.584, 0.609, 0.644, and 0.741  $M_{\odot}$ , respectively, Althaus et al. 2009). The black lines indicate when the initial C abundance has dropped by a factor of two (solid line) and a factor of ten (dashed line, Unglaub & Bues 2000).

(2013) for Fe v is correct and can be generalised to J0536+5448 then the variation of the fine structure constant could be as large as  $1 \times 10^{-4}$ . This is 2.5 times larger the Berengut et al. (2013) estimate for G191–B2B using Fe v ( $4.2 \pm 1.6 \times 10^{-5}$ ). A successful detection of such a variation would be the first direct measurement of a gravitational field effect on a bare constant of nature.

## ACKNOWLEDGEMENTS

NR is supported by a research fellowship of the Royal Commission for the Exhibition of 1851. SG acknowledges funding by the Heisenberg program of the Deutsche Forschungsgemeinschaft under grant GE 2506/8-1. This research has made use of NASA's Astrophysics Data System, the VizieR catalogue access tool and the SIMBAD data base operated at CDS, Strasbourg, France. The TheoSSA service (<http://dc.g-vo.org/theossa>) and TMAD service (<http://astro.uni-tuebingen.de/~TMAD/>) used to retrieve theoretical spectra and model atoms for this paper were constructed as part of the activities of the German Astrophysical Virtual Observatory. This work has made use of data from the European Space Agency (ESA) mission *Gaia* (<https://www.cosmos.esa.int/gaia>), processed by the *Gaia* Data Processing and Analysis Consortium (DPAC, <https://www.cosmos.esa.int/web/gaia/dpac/consortium>). Funding for the DPAC has been provided by national institutions, in particular the institutions participating in the *Gaia* Multilateral Agreement.

## REFERENCES

- Ahn C. P., et al., 2012, *ApJS*, **203**, 21
- Althaus L. G., Serenelli A. M., Panei J. A., Córscico A. H., García-Berro E., Scóccola C. G., 2005, *A&A*, **435**, 631
- Althaus L. G., Panei J. A., Miller Bertolami M. M., García-Berro E., Córscico A. H., Romero A. D., Kepler S. O., Rohrmann R. D., 2009, *ApJ*, **704**, 1605
- Bainbridge M., et al., 2017, *Universe*, **3**, 32
- Berengut J. C., Flambaum V. V., Ong A., Webb J. K., Barrow J. D., Barstow M. A., Preval S. P., Holberg J. B., 2013, *Physical Review Letters*, **111**, 010801
- Bianchi L., Conti A., Shiao B., 2014, VizieR Online Data Catalog, **2335**, 0
- Chambers K. C., et al., 2016, preprint, ([arXiv:1612.05560](https://arxiv.org/abs/1612.05560))
- Cohen M., Megeath S. T., Hammersley P. L., Martín-Luis F., Stauffer J., 2003, *AJ*, **125**, 2645
- Cutri R. M., et al. 2014, VizieR Online Data Catalog, **2328**, 0
- Dreizler S., Heber U., 1998, *A&A*, **334**, 618
- Dreizler S., Werner K., 1996, *A&A*, **314**, 217
- Dreizler S., Heber U., Napiwotzki R., Hagen H. J., 1995, *A&A*, **303**, L53
- Fitzpatrick E. L., 1999, *PASP*, **111**, 63
- Gaia Collaboration et al., 2016, *A&A*, **595**, A1
- Gaia Collaboration Brown A. G. A., Vallenari A., Prusti T., de Bruijne J. H. J., Babusiaux C., Bailer-Jones C. A. L., 2018, preprint, ([arXiv:1804.09365](https://arxiv.org/abs/1804.09365))
- Gianninas A., Bergeron P., Dupuis J., Ruiz M. T., 2010, *ApJ*, **720**, 581
- Green G. M., et al., 2014, *ApJ*, **783**, 114
- Green G. M., et al., 2018, preprint, ([arXiv:1801.03555](https://arxiv.org/abs/1801.03555))
- Henden A. A., Templeton M., Terrell D., Smith T. C., Levine S., Welch D., 2016, VizieR Online Data Catalog, **2336**
- Hirsch H. A., 2009, PhD thesis, University Erlangen-Nürnberg
- Holberg J. B., Bergeron P., 2006, *AJ*, **132**, 1221
- Hoyer D., Rauch T., Werner K., Kruk J. W., Quinet P., 2017, *A&A*, **598**
- Hoyer D., Rauch T., Werner K., Kruk J. W., 2018, preprint, ([arXiv:1801.02414](https://arxiv.org/abs/1801.02414))
- Hügelmeier S. D., Dreizler S., Homeier D., Krzesiński J., Werner K., Nitta A., Kleinman S. J., 2006, *A&A*, **454**, 617
- Iben Jr. I., Kaler J. B., Truran J. W., Renzini A., 1983, *ApJ*, **264**, 605
- Krzesiński J., Kleinman S. J., Nitta A., Hügelmeier S., Dreizler S., Liebert J., Harris H., 2009, *A&A*, **508**, 339
- Lawrence A., et al., 2013, VizieR Online Data Catalog, **2319**, 0
- Miller Bertolami M. M., 2014, *A&A*, **562**, A123
- Miller Bertolami M. M., Althaus L. G., Unglaub K., Weiss A., 2008, *A&A*, **491**, 253
- Miller Bertolami M. M., Melendez B. E., Althaus L. G., Isern J., 2014, ArXiv e-prints 1406.7712,
- Napiwotzki R., 1999, *A&A*, **350**, 101
- Preval S. P., Barstow M. A., Holberg J. B., Barrow J., Berengut J., Webb J., Dougan D., Hu J., 2015, in Dufour P., Bergeron P., Fontaine G., eds, *Astronomical Society of the Pacific Conference Series Vol. 493*, 19th European Workshop on White Dwarfs. p. 415 ([arXiv:1410.0809](https://arxiv.org/abs/1410.0809))
- Rauch T., Deetjen J. L., 2003, in Hubeny I., Mihalas D., Werner K., eds, *Astronomical Society of the Pacific Conference Series Vol. 288*, *Stellar Atmosphere Modeling*. p. 103 ([arXiv:astro-ph/0403239](https://arxiv.org/abs/astro-ph/0403239))
- Rauch T., Werner K., Biéumont É., Quinet P., Kruk J. W., 2012, *A&A*, **546**, A55
- Rauch T., Werner K., Quinet P., Kruk J. W., 2014a, *A&A*, **564**, A41
- Rauch T., Werner K., Quinet P., Kruk J. W., 2014b, *A&A*, **566**, A10
- Rauch T., Werner K., Quinet P., Kruk J. W., 2015a, *A&A*, **577**, A6
- Rauch T., Hoyer D., Quinet P., Gallardo M., Raineri M., 2015b, *A&A*, **577**, A88
- Rauch T., Quinet P., Hoyer D., Werner K., Demleitner M., Kruk J. W., 2016, *A&A*, **587**, A39
- Rauch T., Gamrath S., Quinet P., Löbbling L., Hoyer D., Werner K., Kruk J. W., Demleitner M., 2017a, *A&A*, **599**, A142
- Rauch T., Quinet P., Knörzer M., Hoyer D., Werner K., Kruk J. W., Demleitner M., 2017b, *A&A*, **606**, A105
- Reindl N., Rauch T., Werner K., Kepler S. O., Gänsicke B. T., Gentile Fusillo N. P., 2014, *A&A*, **572**, A117
- Schuh S., et al., 2008, *Astronomische Nachrichten*, **329**, 376
- Sion E. M., 2011, *Hot White Dwarfs*. WILEY-VCH, p. 1
- Unglaub K., Bues I., 2000, *A&A*, **359**, 1042
- Werner K., Herwig F., 2006, *PASP*, **118**, 183
- Werner K., Rauch T., 2014, *A&A*, **569**, A99
- Werner K., Dreizler S., Heber U., Rauch T., Wisotzki L., Hagen H.-J., 1995, *A&A*, **293**, L75
- Werner K., Deetjen J. L., Dreizler S., Nagel T., Rauch T., Schuh S. L., 2003, in Hubeny I., Mihalas D., Werner K., eds, *Astronomical Society of the Pacific Conference Series Vol. 288*, *Stellar Atmosphere Modeling*. p. 31 ([arXiv:astro-ph/0209535](https://arxiv.org/abs/astro-ph/0209535))
- Werner K., Dreizler S., Rauch T., 2012, TMAP: Tübingen NLTE Model-Atmosphere Package, Astrophysics Source Code Library (ascl:1212.015)
- Werner K., Rauch T., Kepler S. O., 2014, *A&A*, **564**, A53
- Zhang X., Jeffery C. S., 2012a, *MNRAS*, **419**, 452
- Zhang X., Jeffery C. S., 2012b, *MNRAS*, **426**, L81
- Zinn J. C., Pinsonneault M. H., Huber D., Stello D., 2018, preprint, ([arXiv:1805.02650](https://arxiv.org/abs/1805.02650))

This paper has been typeset from a  $\text{\TeX}/\text{\LaTeX}$  file prepared by the author.